Proceedings of the 1997 IEEE
International Conference on Robotics and Automation
Albuquerque, New Mexico - April 1997

Vibration Suppression Control of Constrained Spatial Flexible Manipulators

Jin-Soo Kim*, Kuniaki Suzuki**, Mitsuhiro Yamano* and Masaru Uchiyama*

*Department of Aeronautics and Space Engineering, Tohoku University
Aramaki-aza-Aoba, Aoba-ku, Sendai 980-77, Japan
** Tohoku Electric Power Company,
3-7-1 ichibancho, Aoba-ku, Sendai, Japan

Abstract

For free motions, vibration suppression of flexible manipulators has been one of the hottest research topics. However, for constrained motions, a little effort has been devoted for vibration suppression control. Using the dependency of elastic deflections of links on contact force under static conditions, vibrations for constrained planar two-link flexible manipulators have been suppressed successfully by controlling the contact force. However, for constrained spatial multi-link flexible manipulators, the vibrations cannot be suppressed by only controlling the contact force. So, the aim of this paper is to clarify the vibration mechanism of a constrained, multi-DOF, flexible manipulator and to devise the suppression method. We apply a concise hybrid position/force control scheme to control a flexible manipulator modeled by lumped-parameter modeling method. Finally, a comparison between simulation and experimental results is presented to show the performance of our method.

1. Introduction

The effect of flexibility on trajectory tracking performance and compensation of structural compliance has been the subject of a number of publications for manipulator's non-contact task execution [1]. But the same for contact task execution is rarely found. Recently, some researchers have started the study of position/force control of flexible manipulators, and some experiments have been conducted. These researches are mainly for constrained planar flexible manipulators with one or two elastic links, for their modeling and stability analysis [2]~[6]. However, so far only a few attempts have been made for position/force control of multi-DOF, spatial constrained flexible manipulators [7].

For free motions of end-effector, vibration suppres-sion of flexible manipulators has been one of the hottest research topics, but for constrained motions, a little work has been done on vibration suppression control. We have already pointed out that application of vibration control scheme is not necessary due to dependency of elastic deflections of links on the contact force. So, vibrations for a constrained planar two-link flexible manipulator have been successfully suppressed by controlling the contact force [4].

However, for constrained spatial multi-link flexible manipulators, the vibrations cannot be suppressed by only controlling the contact force. So, for such manipulators, the vibration suppression control scheme is also necessary to be included in the control loop.

In this paper, we aim at clarifying the vibration mechanism and proposing the vibration suppression control scheme for a constrained, multi-DOF, flexible manipulator. We apply Hamilton's principle and the lumped-parameter modeling method [8] to establish the dynamic equations and the relations of elastic deflections of links with contact force. A precise simulation model is also developed using the commercial dynamic analysis software package ADAMS™. Finally, experiments and simulations are performed, and a comparison of the results is given to show the performance of our method.

2. Dynamic Modeling of Constrained Flexible Manipulators

In this paper, we assume a flexible manipulator described by the generalized coordinates q

$$q = \begin{bmatrix} \theta^T & e^T \end{bmatrix}^T,$$

where, $\theta \in \Re^n$ is the vector of the joint angles and $e \in \Re^m$ is the vector of the elastic deflections. We further assume that this flexible manipulator is set to an environmental constraint which is only rheonomous

and can be expressed in the following form

$$\varphi(\boldsymbol{q}, t) = 0, \tag{1}$$

where $\varphi : \Re^{n+m} \to \Re^1$ is a smooth constraint function, and t is time. Using a lumped-parameter model of the flexible manipulator, the equations of motion can be derived based on the Hamilton's principle, and can be written as

$$\boldsymbol{\tau} = \boldsymbol{M}_{11}(\boldsymbol{q})\ddot{\boldsymbol{\theta}} + \boldsymbol{M}_{21}(\boldsymbol{q})\ddot{\boldsymbol{e}} + \boldsymbol{h}_1(\boldsymbol{q}, \dot{\boldsymbol{q}})$$
$$+ \boldsymbol{g}_1(\boldsymbol{q}) + \boldsymbol{j}_{\varphi\theta}^T(\boldsymbol{q})\lambda, \tag{2}$$

$$0 = \boldsymbol{M}_{12}(\boldsymbol{q})\ddot{\boldsymbol{\theta}} + \boldsymbol{M}_{22}(\boldsymbol{q})\ddot{\boldsymbol{e}} + \boldsymbol{h}_2(\boldsymbol{q}, \dot{\boldsymbol{q}})$$
$$+ \boldsymbol{K}_{22}\boldsymbol{e} + \boldsymbol{g}_2(\boldsymbol{q}) + \boldsymbol{j}_{\varphi e}^T(\boldsymbol{q})\lambda, \tag{3}$$

where $\boldsymbol{M}_{11} \in \Re^{n \times n}$, $\boldsymbol{M}_{12} \in \Re^{n \times m}$, $\boldsymbol{M}_{21} \in \Re^{m \times n}$ and $\boldsymbol{M}_{22} \in \Re^{m \times m}$ are submatrices of the inertia matrix. $\boldsymbol{h}_1$ and $\boldsymbol{h}_2$ are vectors of centrifugal and Coriolis forces, $\boldsymbol{g}_1$ and $\boldsymbol{g}_2$ are gravity vectors, $\boldsymbol{K}_{22} \in \Re^{m \times m}$ is stiffness matrix, $\lambda \in \Re^1$ is the Lagrange multiplier, $\boldsymbol{j}_{\varphi\theta}$ and $\boldsymbol{j}_{\varphi e}$ are constraint Jacobian matrices, and $\boldsymbol{\tau} \in \Re^n$ is the joint torque vector. The equations of motion have two distinct parts, one is related to the overall motion of the system (Eq. (2)), while the other is related to the elastic motion only (Eq. (3)).

Here, we use the Jacobian matrix for the above rheonomous constraint as

$$\boldsymbol{j}_\varphi = \frac{\partial \varphi}{\partial \boldsymbol{p}} \boldsymbol{j}_q(\boldsymbol{q})$$
$$= \left[\begin{array}{cccccccc} \frac{\partial \varphi}{\partial \theta_1} & \frac{\partial \varphi}{\partial \theta_2} & \cdots & \frac{\partial \varphi}{\partial \theta_n} & \frac{\partial \varphi}{\partial e_1} & \frac{\partial \varphi}{\partial e_2} & \cdots & \frac{\partial \varphi}{\partial e_m} \end{array} \right]$$
$$= \left[\begin{array}{cc} \boldsymbol{j}_{\varphi\theta} & \boldsymbol{j}_{\varphi e} \end{array} \right], \tag{4}$$

where $\boldsymbol{j}_q = [\boldsymbol{j}_\theta \ \boldsymbol{j}_e]$ is the conventional Jacobian matrix of the manipulator, and $\boldsymbol{p}$ represents the Cartesian coordinates and the three Euler angles for end-effector. The Lagrange multiplier can be represented as

$$\lambda = \frac{f_n}{|\text{grad}\varphi|},$$
$$\text{grad}\varphi = \boldsymbol{\nabla}\varphi = \frac{\partial \varphi}{\partial \boldsymbol{p}}, \tag{5}$$

where f_n is the component of the contact force normal to the constraint environment.

In order to simplify Eq. (2) and Eq. (3), we make the following assumptions:

- The centrifugal and Coriolis terms are small enough to be ignored.

- The influence of elastic deflections e is small enough to approximate $\boldsymbol{M}_{ij}(\boldsymbol{q})$ and $\boldsymbol{g}_{ij}(\boldsymbol{q})$ as $\boldsymbol{M}_{ij}(\boldsymbol{\theta})$ and $\boldsymbol{g}_{ij}(\boldsymbol{\theta})$ $(i = 1, 2; j = 1, 2)$ respectively.

Then, Eqs. (2) and (3) can be rewritten in the following compact form

$$\boldsymbol{L}\boldsymbol{\tau} = \boldsymbol{M}(\boldsymbol{\theta})\ddot{\boldsymbol{q}} + \boldsymbol{K}\boldsymbol{q} + \boldsymbol{g}(\boldsymbol{\theta}) + \boldsymbol{j}_\varphi^T(\boldsymbol{q})\lambda, \tag{6}$$

where

$$\boldsymbol{L} = \left[\begin{array}{c} \boldsymbol{I}_n \\ \boldsymbol{0}_{m \times n} \end{array} \right], \quad \boldsymbol{K} = \left[\begin{array}{cc} \boldsymbol{0}_{n \times n} & \boldsymbol{0}_{n \times m} \\ \boldsymbol{0}_{m \times n} & \boldsymbol{K}_{22} \end{array} \right].$$

3. Vibration Mechanism

For a particular constrained motion of a spatial flexible manipulator, the joints which have their axis of rotation normal to the constraint environment, can get their constraint Jacobian of $j_{\varphi\theta p}$ $(p = 1, 2 \cdots n)$ close to zero for constrained workspace, that is, the influence of contact force $(j_{\varphi\theta p}\lambda)$ for those joints almost disappears. Thus, vibrations due to motions of those particular joints take no influence of contact force, that is, $j_{\varphi e q}\lambda$ of Eq. (3) is also close to zero $(q = 1, 2 \cdots m)$. Since λ is not zero, the only thing which can be approximated to zero is the Jacobian for deflection constraint $j_{\varphi e q}$.

Therefore, Eq. (6) can be decomposed into two separate equations as follows

$$\boldsymbol{L}_c\boldsymbol{\tau}_c = \boldsymbol{M}_c(\boldsymbol{\theta})\ddot{\boldsymbol{q}}_c + \boldsymbol{K}_c\boldsymbol{q}_c + \boldsymbol{g}_c(\boldsymbol{\theta}) + \boldsymbol{j}_{\varphi c}^T(\boldsymbol{q})\lambda, \tag{7}$$
$$\boldsymbol{L}_f\boldsymbol{\tau}_f = \boldsymbol{M}_f(\boldsymbol{\theta})\ddot{\boldsymbol{q}}_f + \boldsymbol{K}_f\boldsymbol{q}_f + \boldsymbol{g}_f(\boldsymbol{\theta}). \tag{8}$$

- Eq. (7) gives the dynamics of subsystem which observes an influence of constraint (contact force, in other words) on its movements and deflections. This is named as "Constrained motion subsystem "[subscript c].

- Eq. (8) gives the dynamics of subsystem which observes no influence of contact force on its movements and deflections. This is named as "Free motion subsystem "[subscript f].

In the stationary condition (i.e., $\ddot{\boldsymbol{\theta}} = \dot{\boldsymbol{\theta}} = \boldsymbol{0}$ and $\ddot{\boldsymbol{e}} = \dot{\boldsymbol{e}} = \boldsymbol{0}$), Equations (7) and (8) can be rewritten as

$$0 = \boldsymbol{K}_{22c}\boldsymbol{e}_{0c} + \boldsymbol{g}_{2c} + \boldsymbol{j}_{\varphi e}^T\lambda, \tag{9}$$
$$0 = \boldsymbol{K}_{22f}\boldsymbol{e}_{0f} + \boldsymbol{g}_{2f}, \tag{10}$$

where $\boldsymbol{e}_{0f}$ is the static deflection due to both gravity and contact force, while $\boldsymbol{e}_{0c}$ is static deflection due to gravity only. Therefore we can conclude that

- For constrained motion subsystem, vibration control scheme is not necessary due to dependency of elastic deflections of links on the contact force.
- For free motion subsystem, vibration control scheme is necessary as it has got its movements and deflections same as those for a free motion of end-effector.

4. Hybrid Position/Force Control Scheme

For a manipulator equipped with velocity feedback servo motors, the relationship between the velocity commands and the produced torques can be written as

$$\tau = G_r K_{sp}(V_{ref} - K_{sv}\dot{\theta}_m)$$
$$= \Lambda(\dot{\theta}_{com} - \dot{\theta}), \tag{11}$$

where

G_r	:	gear reduction ratios,
K_{sp}	:	voltage feedback gains,
K_{sv}	:	voltage/velocity coefficients,
$\dot{\theta}_m = G_r\dot{\theta}$	:	angular velocities of motors,
V_{ref}	:	voltage velocity commands,
$\dot{\theta}_{com}$	:	velocity commands, and
$\Lambda = G_r{}^2 K_{sp}K_{sv}$	:	velocity feedback gains.

The voltage velocity commands V_{ref} are computed by

$$V_{ref} = G_r K_{sv}\dot{\theta}_{com}, \tag{12}$$

and are used in the experiments.

4.1. Vibration suppression

Now, we propose a method to find the term $\dot{\theta}_e$ that suppresses the vibrations of the robot [9] [10]. The effect of a stiff velocity servo loop on the equations of motion (Eq. (2)) is to transform the relation $\dot{\theta} = \dot{\theta}_{com}$. Then, in Eq. (3), the acceleration can be considered as an input $\ddot{\theta}_e$ to the dynamics of deflections. Therefore, elastic motion of Eq. (8) can be written as

$$M_{22f}(\theta)\Delta\ddot{e}_f + K_{22f}\Delta e_f = -M_{21f}(\theta)\ddot{\theta}_e, \tag{13}$$

where

$$\Delta e_f = e_f - e_{0f} = e_f - K_{22f}^{-1}g_{2f}.$$

Suppose that we want to transform Eq. (13) into an ideal stable system

$$\Delta\ddot{e}_f + K_v\Delta\dot{e}_f + K_v\Delta e_f = 0, \tag{14}$$

where

K_v is a diagonal velocity gain matrix,
K_p is a diagonal position gain matrix.
This can be accomplished if

$$-M_{21f}(\theta)\ddot{\theta}_e = M_{22f}(\theta)[-K_v\Delta\dot{e}_f - K_p\Delta e_f]$$
$$+ K_{22f}\Delta e_f. \tag{15}$$

To calculate $\ddot{\theta}_e$, $M_{21}(\theta)$ needs to be inverted. Nevertheless this is only possible if the number of joint rotations is equal to the number of elastic deflections ($n = m$).

But as, generally, $n < m$, so an approximate solution can be obtained using the Moore-Penrose pseudoinverse to minimize the error in Eq. (15)

$$\ddot{\theta}_e = M_{21f}^+(\theta)\{M_{22f}(\theta)[K_v\Delta\dot{e}_f + K_p\Delta e_f]$$
$$- K_{22f}\Delta e_f\}. \tag{16}$$

If we consider only the inertial decoupling of Eq. (13), Eq. (16) can be transformed into the simplified law as

$$\ddot{\theta}_e = M_{21f}^+(\theta)M_{22f}(\theta)[K_v\Delta\dot{e}_f + K_p\Delta e_f]. \tag{17}$$

Integrating it for a given θ we can have

$$\dot{\theta}_e = K_{ep}\Delta e_f + K_{ei}\int_0^t \Delta e_f, \tag{18}$$

where

$$K_{ep}(\theta) = M_{21f}^+(\theta)M_{22f}(\theta)K_v,$$
$$K_{ei}(\theta) = M_{21f}^+(\theta)M_{22f}(\theta)K_p. \tag{19}$$

4.2. Velocity command

The approximate joint velocities for constrained motion subsystem $\dot{\theta}_{com}$ can be computed as

$$\dot{\theta}_{com} = \dot{\theta}_t + \dot{\theta}_f, \tag{20}$$

and for free motion subsystem as

$$\dot{\theta}_{com} = \dot{\theta}_t + \dot{\theta}_e, \tag{21}$$

where $\dot{\theta}_t$ is the joint velocity vector for positioning and $\dot{\theta}_f$ is an additional component for force control. The velocities $\dot{\theta}_t$, $\dot{\theta}_f$ and $\dot{\theta}_e$ are respectively computed as

$$\dot{\theta}_t = j_\theta^{-1}(I - n^T n)[K_{tp}(p_d - p) + K_{ti}\int_0^t (p_d - p)],$$

$$\dot{\theta}_f = \Lambda^{-1}j_\theta^T n^T[K_{fp}(f_d - f_n) + K_{fi}\int_0^t (f_d - f_n)],$$

$$\dot{\theta}_e = K_{ep}\Delta e + K_{ei}\int_0^t \Delta e, \tag{22}$$

where I is the unit matrix, and $n = \dfrac{\nabla\varphi}{|\nabla\varphi|}$ is the unit vector normal to the constraints. n^T, $(I - n^T n)$ define matrices which respectively select the directions for application of force and end-effectors motion.
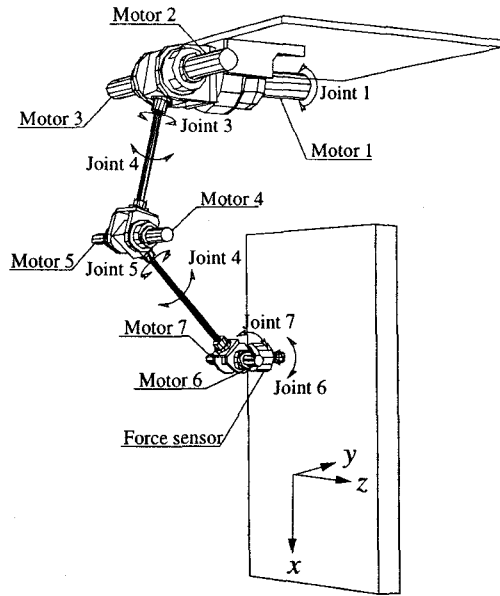
2833

Figure 1. Experimental robot with 2 links and 7 joints.

5. Application of the Proposed Scheme

To clarify the discussion, the constrained motions of an experimental flexible manipulator ADAM (Aerospace Dual Arm Manipulator) are considered. ADAM has two arms, each of which consists of 2 elastic links and 7 rotory joints [11]. In this paper, however, only the left arm (Fig. 1) is considered. The discussion is restricted to motions of joints 1, 2, 4 and 6 only while joint 6 always preserves an angle of $\pi/2$ [rad], for end-effector with respect to the constraint environment. The constraint is a vertical plane located at 0.375 [m] in the y direction from the robot's reference coordinates. So, the end-effector is constrained in only the y direction, whereas it is free to move in the $x - z$ plane.

Experiments and simulations are performed. The results achieved by a precise model designed by the commercial dynamic analysis software package ADAMS$^{\mathrm{TM}}$, are compared with the experimental results.

5.1. Experimental setup

Our experimental manipulator ADAM is driven by DC servo motors with velocity feedback control. The tip deflections of each link of this manipulator are computed from link's strains measured by strain gauges located at the root of each link while a wrist force/torque sensor is used to measure the contact force at end-effector. The parameters of each link are presented in Table 1.

Table 1. ADAM link parameters.

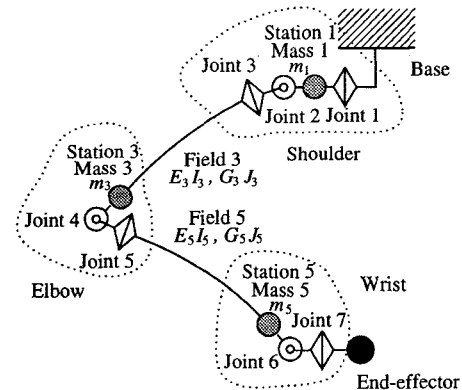|	Link 3	Link 5
Length	0.5 m	0.5 m
Elastic part	0.359 m	0.394 m
Diameter	0.013 m	0.01 m
Material	SUP-6	SUP-6
EI	288.1 Nm^2	100.8 Nm^2
GJ	224.32 Nm^2	78.54 Nm^2
Mass	0.7 kg	0.5 kg

Figure 2. Lumped-parameter model of the experimental manipulator ADAM.

5.2. Modeling of ADAM

The arm under consideration is modeled by lumped-masses and massless springs as shown in Fig. 2 [8]. The lumped masses (*stations*) are considered concentrated at the tips of the respective links while the links themselves are considered as massless springs (*fields*) with elastic and torsional properties as $E_3 I_3$, $E_5 I_5$ and $G_3 J_3$, $G_5 J_5$, respectively. The joint angle vector θ and the link deflection vector e are:

$$\theta = \begin{bmatrix} \theta_1 & \theta_2 & \theta_4 \end{bmatrix}^T, \tag{23}$$

$$e = \begin{bmatrix} \delta_{y3} & \delta_{z3} & \delta_{y5} & \delta_{z5} \end{bmatrix}^T. \tag{24}$$

where δ_{y3}, δ_{y5}, δ_{z3} and δ_{z5} are elastic deflections along the y and z axes of links 3 and 5, respectively.

5.3. A precise simulation model

A precise model of the ADAM robot is constructed by ADAMS$^{\mathrm{TM}}$. In this simulator, a finite-element method based on Timosenko beam theory is used as a modeling method for flexible structures. We consider our experimental manipulator as having 5 beam elements. A simple model of Coulomb friction is included in order to obtain a realistic simulation model reflecting the experimental conditions. When the end-effector velocities become -0.001 [m/s] and 0.001 [m/s],
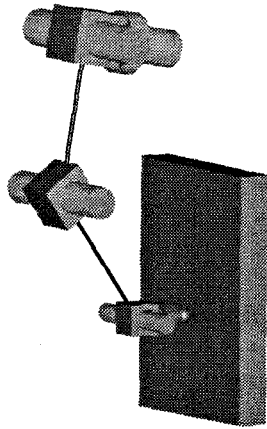
2834

Figure 3. ADAMS™ simulation model.

friction forces become $-\mu f_n$ [N] and μf_n [N], respectively, where μ is the friction constant. This friction model is recommended to be used for ADAMS™.

6. Experiments and Simulations

The constraint equation can be written as

$$\varphi = y - 0.375. \tag{25}$$

For constraint workspace, $\mathbf{j}_\varphi$ of Eq. (4) for ADAM are given as follows and shown in Fig. 4.

$$\mathbf{j}_\varphi = \left[\begin{array}{ccccccc} \dfrac{\partial \varphi}{\partial \theta_1} & \dfrac{\partial \varphi}{\partial \theta_2} & \dfrac{\partial \varphi}{\partial \theta_4} & \dfrac{\partial \varphi}{\partial \delta_{y3}} & \dfrac{\partial \varphi}{\partial \delta_{z3}} & \dfrac{\partial \varphi}{\partial \delta_{y5}} & \dfrac{\partial \varphi}{\partial \delta_{z5}} \end{array} \right]$$

$$= \left[\begin{array}{ccccccc} j_{\varphi\theta1} & j_{\varphi\theta2} & j_{\varphi\theta4} & j_{\varphi e1} & j_{\varphi e2} & j_{\varphi e3} & j_{\varphi e4} \end{array} \right].$$

It can be noted that the horizontal motion of manipulator $(\theta_1, \delta_{z3}, \delta_{z5})$ is a free motion while the vertical motion $(\theta_2, \theta_3, \delta_{z3}, \delta_{z5})$ is constrained one. In Eqs. (7) and (8), $\mathbf{q}_c, \mathbf{\tau}_c, \mathbf{q}_f, \mathbf{\tau}_f$ become

$$\mathbf{q}_c = \left[\begin{array}{c} \theta_2 \\ \theta_4 \\ \delta_{y3} \\ \delta_{y5} \end{array} \right], \quad \mathbf{q}_f = \left[\begin{array}{c} \theta_1 \\ \delta_{z3} \\ \delta_{z5} \end{array} \right],$$

$$\mathbf{\tau}_c = \left[\begin{array}{c} \tau_2 \\ \tau_{z4} \end{array} \right], \quad \mathbf{\tau}_f = \left[\begin{array}{c} \tau_1 \end{array} \right]. \tag{26}$$

In this section, we will study vibrations of the constrained manipulator using simulation and experimental results. The simulations and experiments are performed for the following cases;

- End-effector is moving in y direction without vibration suppression (Fig. 5),
- End-effector is moving in z direction without vibration suppression (Fig. 6),
- End-effector is moving in z direction with vibration suppression (Fig. 7).

For these simulations, K_{sp} of Eq. (11) is decided to be approximated to the one used in the experiments. The environmental stiffness and friction constants are taken as 10000 [N/m] and 0.2, respectively. The sampling time and the desired contact force are set as 10 [ms] and 10 [N] respectively. In the experiments and simulations, we set $K_{tp} = 4I_3[1/s]$, $K_{ti} = 0I_3[1/s^2]$, $K_{fp} = 0.4[m]$, $K_{fi} = 0[m/s]$, $K_v = 0I_3$, $K_p = 0I_3[1/s]$ for the first and the second cases, while $K_{tp} = 4I_3[1/s]$, $K_{ti} = 0I_3[1/s^2]$, $K_{fp} = 0.4[m]$, $K_{fi} = 0[m/s]$, $K_v = 32I_3$, $K_p = 0I_3[1/s]$ for the third case only.

Fig. 5 shows the responses of experimental and simulation results for the first case. In this case, the velocity command is given by Eq. (20) as it is the case of constrained motion subsystem. From Fig. 5, we can see that the vibrations of end-effector are suppressed by controlling the contact force only.

Next, let us study the free motion subsystem. Fig. 6 shows the responses of experimental and simulation results for the second case. Using Eq. (20) for the velocity command of horizontal motion, it is clear that the vibrations cannot be suppressed by controlling the contact force only. It means that the vibrations in the direction of motion take no influence of contact force. So, such motions are like free motions of the system.

Thus, the vibration suppression control loop is necessary to be included in the velocity command, expressed in Eq. (21). Fig. 7 shows that the vibrations are successfully suppressed by including the vibration suppression control loop. In this case, velocity commands of joints 1 and 2 are given by Eq. (20) whereas the one for joint 4 is given by Eq. (21). So, the same effect of vibration suppression can be achieved by using the velocity commands for all joints including vibration suppression control loop.

7. Conclusions

The vibration mechanism and vibration suppression for constrained spatial flexible manipulators has been presented. A constrained spatial flexible manipulator system can be divided into constrained motion subsystem and free motion subsystem for a particular task execution, but there exists no free motion subsystem for a constrained planar manipulator. The concept of free and constrained motion subsystem seems to be interesting for an efficient task execution .

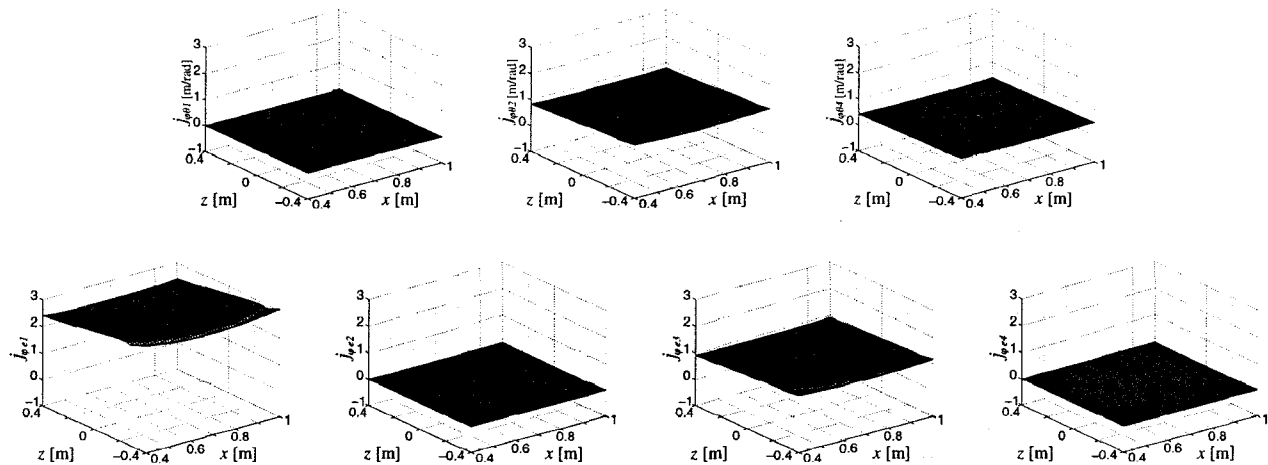The control scheme has been studied for a 2-link 7-

2835

Figure 4. Constraint Jacobian.

joint type manipulator. Experiments and simulations have been conducted and their results show the effectiveness of the scheme.

References

[1] A. Konno and M. Uchiyama, "VIBRATION SUPPRESSION CONTROL OF SPATIAL FLEXIBLE MANIPULATORS," *Control Engineering Practice, A Journal of IFAC*, Vol. 3, No. 9, pp. 1315–1321, 1995.

[2] B. C. Chiou and M. Shahinpoor, "Dynamics Stability Analysis of a Two-Link Force-Controlled Flexible Manipulator," Trans. ASME, J. of Dynamic System, Measurement and control, vol. 112, pp. 661–666, 1990.

[3] F. Matsuno T. Asano and Y. Sakawa, "Modeling and Quasi-Static Hybrid Position/Force Control of a Constrained Planar Two-Link Flexible Manipulator," *IEEE Trans. on Robotics and Automation*, vol. 10, no. 3, pp. 287–297, 1994.

[4] J. S. Kim, K. Suzuki, A. Konno and M. Uchiyama, "Force Control of Constrained Flexible Manipulators," *Proc. of the IEEE Int. Conf. on Robotics and Automation*, Vol. 1, pp. 635–640, 1996.

[5] P. Rocco and W. J. Book, "Modelling for two-time scale Force/Position Control of Flexible Robots," *Proc. of the IEEE Int. Conf. on Robotics and Automation*, Vol. 1, pp. 1941–1945, 1996.

[6] D. Bossert, U. L. Ly and J. Vagners, "Experimental Evaluation of Robust Reduced-Order Hybrid Position/Force Control on a Two-Link Flexible Manipulator," *Proc. of the IEEE Int. Conf. on Robotics and Automation*, Vol. 1, pp. 2573–2578, 1996.

[7] J. S. Kim, K. Suzuki, M. Yamano and M. Uchiyama, "Hybrid Position/Force Control of Spatial Flexible Manipulators," *Proc. of The 3rd Int. Conf. on Motion and Vibration Control*, Vol. 1, pp. 222–227, 1996.

[8] A. Konno and M. Uchiyama, "Modeling of a Flexible Manipulator Dynamics Based upon Holzer's Model," *In Proc. of IEEE/RSJ Int. Conf on intelligent Robots and Systems*, vol. 1, pp. 223–229, 1994 (in Japanese).

[9] A. Konno, M. Uchiyama, Y. Kito and M. Murakami, "Vibration Controllability of Flexible Manipulators," *Proc. of the IEEE Int. Conf. on Robotics and Automation*, Vol. 1, pp. 308–314, 1994.

[10] S. López-Linares, A. Konno and M. Uchiyama, "Controllability of Flexible Manipulators," *Pre- prints of the 4th IFAC Symp. on Robot Control '94*, Vol. 2, pp. 509–516, 1994.

[11] M. Uchiyama, A. Konno, T. Uchiyama, and S. Kanda, "Development of a flexible dual-arm manipulator testbed for space robotics," *Proc. of the IEEE Int. Workshop on Intelligent Robotics and Systems'90*, pp. 375–381, Tsuchiura, Japan, 1990.
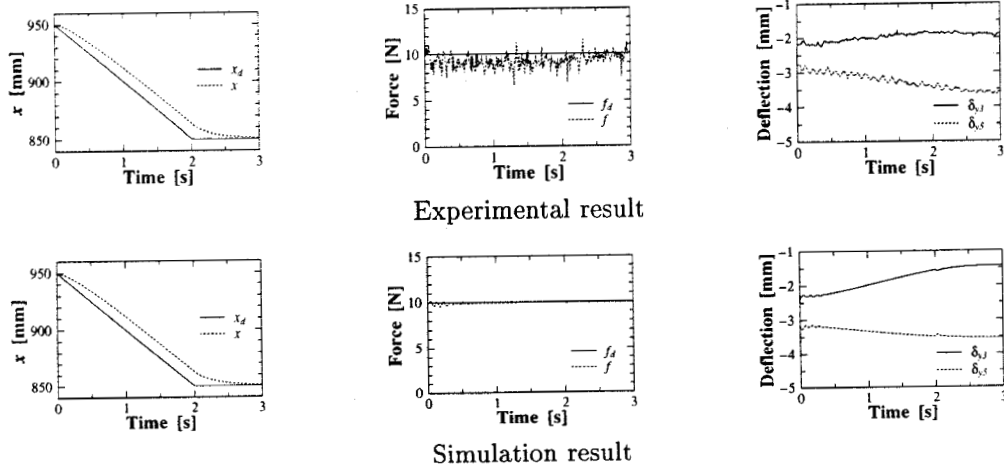
2836

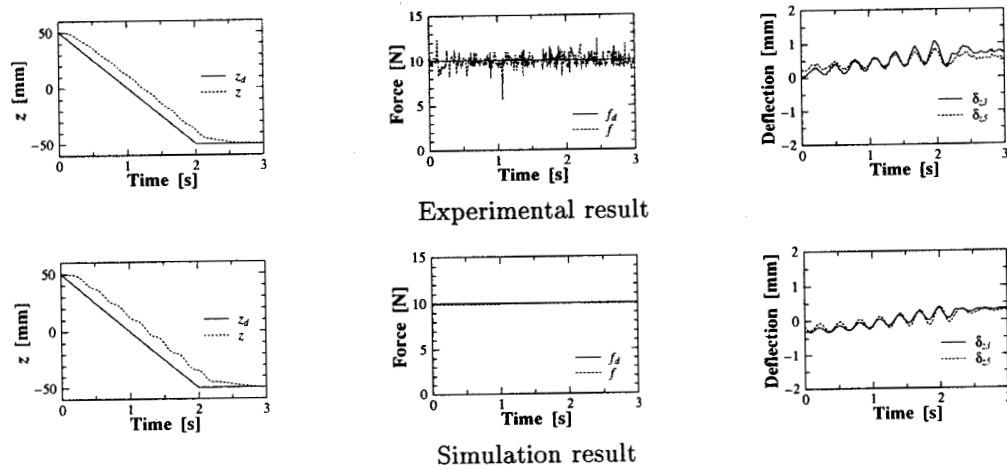Figure 5. End-effector is moving in y direction without vibration suppression.

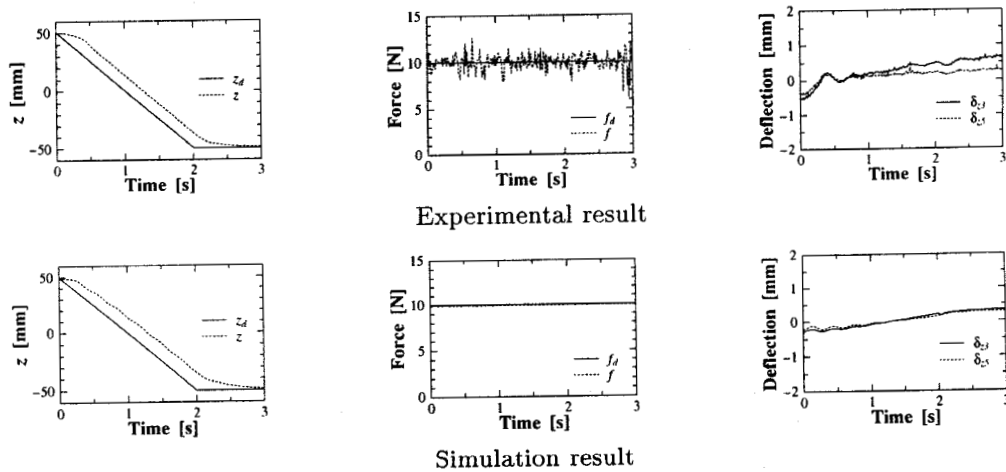Figure 6. End-effector is moving in z direction without vibration suppression.

Figure 7. End-effector is moving in z direction with vibration suppression.